Celal Bayar University Journal of Science

A study on chaotic dynamics of deep artificial neural network activated by biological neuron model

Erdem Erkan[1]*

[1] Computer Engineering Department, Bartin University, 74110 Bartin, Türkiye
* eerkan@bartin.edu.tr
* Orcid No: 0000-0002-2386-1271

Received: 25 August 2024
Accepted: 11 November 2024
DOI: 10.18466/cbayarfbe.1538362

Abstract

This paper analyzes the effects of the chaotic signals used by the brain to perform some cognitive functions on the Spiking Neural Network (SNN), defined as the third-generation Artificial Neural Network (ANN) that best represents the biological neuron. In the first phase of the paper, neural networks with different layers are designed to perform classifications like ANN and SNN. Classification performances of these deep networks using the Rectified Linear Unit activation function in ANN mode and the Izhikevich Neuron model in SNN mode are presented comparatively. It is observed that SNNs perform at least as well as ANNs under normal conditions. In the second stage of the study, the classification performances of these deep networks in the SNN mode were analyzed in different chaotic environments, and the findings were reported. In light of the findings, it is seen that SNNs can exhibit a classification success similar to ANNs and maintain this success rate up to a certain chaotic current intensity. Moreover, some levels of chaotic current contribute to the network's classification performance. This is the first study to investigate the chaotic environment behavior of SNNs.

Keywords: SNN, Izhikevich neuron, Chaotic environment, EEG-Image Classification

1. Introduction

The Artificial Neural Network (ANN) is created by placing units, also called artificial neurons, which are the mathematical representations of the biological neuron in one or more layers. These units use non-linear activation functions such as hyperbolic tangent, sigmoid, and Rectified Linear Unit (ReLu) that make it possible to learn by iteratively changing the weight of each neuron in the network. Since the ANN emerged with Rosenblatt's Perceptron in 1958, ANN has been used in many studies [1]. Although it lost its popularity from time to time, ANNs regained their popularity with two studies conducted in 2009 and 2012. The first is a back propagation ANN study developed for the speech recognition problem [2] and the other is an image classification study AlexNet [3] for estimating the dominant object in the given image. Apart from these, ANNs have been used in pattern recognition, two or multi-class seizure classification, and human-robot interaction systems. It has been reported that the classification performance of ANNs is better than other classification methods in many studies [4]

Although ANNs developed with inspiration from the brain, they do not have an information transmission mechanism that has the firing pattern of a real biological neuron. This mechanism is defined by the Spiking Neural Network (SNN), which is considered to be the third generation ANN and is thought to revolutionize the field in the future [5] SNNs use neuron models expressed with differential equations such as Integrated and Fire [6], Hudking-Huxley [7], Izhikevich [8], FitzHugh-Nagumo [9], Morris-Lecar Neurons [10]. These models frequently used in the field of computational neuroscience are the mathematical equations that best express the biological neuron today. In recent years, more realistic, energy-efficient, and physically applicable machine learning studies have been carried out by the use of these models with machine learning. For example, [11] has presented a state-of-the-art review of the development of spiking neurons and SNNs, and it has provided insight into their evolution through their article [12], introduced a new class of SNN, dynamic eSNN, that utilizes both rank-order learning and dynamic synapses to learn spatial and spectro-temporal data in a fast, on-line mode with their study. Although most of the SNN-based studies are based on image classification [13], there are also studies

on electroencephalography (EEG) classification. In a study, it was compared spiking Neurons with other traditional classifiers commonly used in the recognition of motor imagery tasks [14]. [15] presented brain-inspired SNN architecture to explore the modeling of neural networks underlying the tinnitus symptom by using EEG. In another study, [16] proposed a novel method of using the SNNs and the EEG processing techniques to recognize emotion states. [17] introduced a biologically plausible speech recognition approach by using an unsupervised self-organizing map (SOM) for feature representation and event-driven SNN for spatiotemporal pattern classification. SNNs were also used for acoustic modeling and evaluated their performance in a few vocabulary recognition tasks [18].

In ANNs, the number of layers of the network expresses the depth of the network. For example, AlexNet is known as a deep network consisting of 8 layers and millions of parameters. Equipped with trainable parameters in multiple layers, the deep learning architecture has shown outstanding performance in ANN [19]. The same architecture can be adaptable to SNN. Realizing a deep SNN comparable to traditional Deep Neural Networks (DNN) is a challenge due to hardware constraints. Therefore, the classification performance of SNNs is not as good as the classification performance of DNNs [20].

On the other hand, chaotic regimes induced by the environmental influences in the firing activity of neurons have recently attracted the attention of researchers [21]. In a study, it has been shown that sleep is governed by stable self-sustaining oscillations whereas the silent wake state and active wakefulness state are governed by both disordered oscillations and chaotic dynamics [22]. In [23], it has been noted that the Onchidium Pacemaker neuron exhibits chaotic spiking behavior when exposed to certain periodic signals. With the emergence of chaotic firings in neurons, studies have been conducted in computational neuroscience examining the dynamics of neurons responding to stimuli in a chaotic environment [24]. It has been shown that some cognitive functions in the brain can be performed in the presence of optimal chaotic current. For instance, [25] showed that a bistable system can be steadily designed to certain logic gate operations at the ideal chaotic signal intensity in computational neuroscience. As far as it is known, the chaotic environment behaviors of deep SNNs have not been examined yet. With this motivation, in the first phase of this study, which is carried out in two stages, neural networks with different layers that can classify in ANN and SNN modes are introduced to classify images and brain signals separately. The classification results of these networks are analyzed comparatively in both modes. In the second stage of the study, the classification performances of designed networks activated by Izhikevich neurons in SNN mode were tested in chaotic environments with different chaotic current intensities. The results are compared in both modes of the networks with the same layer structure and the number of neurons. According to the author's best knowledge, this is the first study that investigated the classification success of brain and image signals by using deep SNNs in a chaotic environment.

The remainder of this paper is organized as follows: Section 2 introduces the mathematical structure of the feature extraction method, neuron, and network models. Section 3 includes the comparison of the ANN and SNN modes of the neural networks are designed and gives the classification results of deep biologically capable SNNs in a chaotic environment. Conclusions are drawn in Section 4.

2. Materials and Methods

2.1. Datasets

The methods proposed in this study are tested on two different datasets containing EEG and image data.

2.1.1. ECoG Dataset

The electrocorticography (ECoG) dataset consisting of brain signals was recorded with 64 channels in BCI competition III. During the recording phase, the subject made imaginary movements with his left little finger or tongue. ECoG signals were acquired with electrodes on the contralateral (right) motor cortex, with a 3-second time series and 1000 Hz sampling rate, and amplified to microvolt levels. Every trial consisted of either an imagined tongue or finger movement. The training dataset contains 139 tongue and 139 finger class labeled data [26]. The performances of proposed neural networks were evaluated on the ECoG dataset for motor imaginary tasks.

2.1.2. MNIST Dataset

It is also tested the performance of the neural networks in a digit recognition task. For this reason, data samples were used from the MNIST database, which contains centered, grayscale, 28x28 pixel images of handwritten numbers 0-9 [27]. The training dataset contains 10000 samples, and the test dataset contains 60000 samples. It trained the system with 400 samples of the MNIST dataset in 200 iterations for the 4-digit classification task. MNIST is a numeric character database popularly used for machine learning research. The classes used in the MNIST dataset are given in Figure 1 as a representation.

Celal Bayar University Journal of Science
Volume 20, Issue 4, 2024, p 92-100
Doi: 10.18466/cbayarfbe.1538362

Figure 1. MNIST dataset sample for 4 class

2.2. Continuous Wavelet Transform

Feature extraction of the ECoG dataset is based on Continuous Wavelet Transform (CWT), which is a technique that allows to model variations of an entire signal, within the scale-time domain [28]. Continuous wavelet transform (CWT) is often used in the analysis of time-frequency information for engineering and real-life problems. It is preferred in signal analysis because it preserves time-frequency information. A basis function, named the mother wavelet (ψ(t)) is formulated in Equation 2.1. The s and n represent the scale and position of the signal respectively. Using scaled and dilated forms of the ψ(t), the Continuous Wavelet Transform (CWT) decomposes a finite-energy signal, x(t). The CWT coefficients obtained by decomposing x(t), are given in Equation 2.2. $\psi^*_{s,n}(t)$ denotes the complex conjugate of the mother wavelet function. The x(t) is a finite-energy function, that is, $x(t) \in L^2(R)$. Low-frequency information is obtained at larger scales while high-frequency information is obtained at smaller scales [28].

$$\psi_{s,n}(t) = s^{-1/2}\psi\left(\frac{t-n}{s}\right) \quad \textbf{(2.1)}$$

$$CWT_x(s,n;\psi) = < x(t), \psi_{s,n}(t) > s^{-1/2}\int_{-\infty}^{+\infty} x(t)\psi^*_{s,n}(t)dt \quad \textbf{(2.2)}$$

CWT is used for feature extraction for the ECoG dataset. EEG signals are converted to image format with this method. 2-D time-frequency images called a scalogram, represent the square of CWT. The time-frequency images are used as input for the proposed model.

2.3. Neuron Model (Izhikevich)

The change of the cell membrane potential of the Izhikevich neuron with time is given by Equation 2.3 [8].

$$\frac{dV}{dt} = \frac{k(V-V_r)(V-V_t) - U + pI + \epsilon I_{chaos}}{C} \quad (\mathbf{2.3})$$

$$\frac{dU}{dt} = a(b(V-V_r) - U)$$
$$\text{If } V \geq V_{peak}, \text{ then } V \leftarrow c,\ U \leftarrow U + d \quad \textbf{(2.4)}$$

The V, $C = 100\ \mu F/cm^2$, V_t, V_r, I, U express the membrane potential, the membrane capacitance, the instantaneous threshold potential, the resting membrane potential, the input current, and the recovery current respectively. The model's a, b, c, and d parameters in Equation 2.4 are also expressed as recovery position constant, resistance for input, voltage reset parameter, and the downstroke current during the spike. The $I_{chaos} = \epsilon x$ represents chaotic current. The ϵ is the level of chaotic activity and x is a chaotic signal source [29]:

$$\frac{dx}{dt} = \sigma(y-x), \frac{dy}{dt} = px - y, \frac{dz}{dt} = xz - \lambda z \quad (\mathbf{2.5})$$

The time series of chaotic signal x generated by the Lorenz system and $x-z$ phase plane diagram of the chaotic Lorenz system are given in Figure 2 a and b respectively. It can be seen in Figure 2 that the x signal is in a chaotic oscillation state.

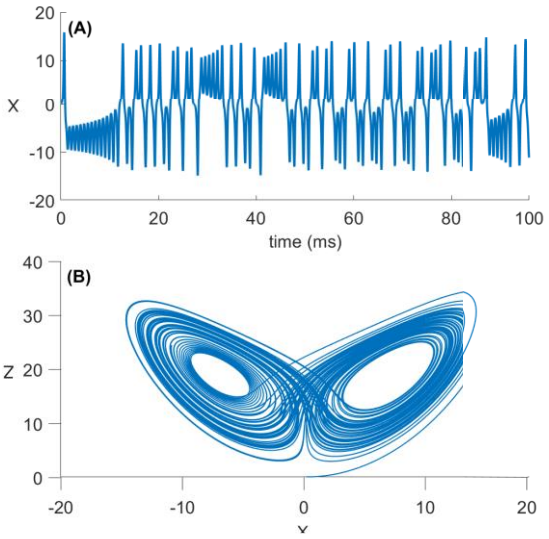

Figure 2. (A) Time series of chaotic signal x ; (B) Phase diagram of chaotic Lorenz system.

The Izhikevich neuron model exhibits different firing patterns at different parameter values. In this study, Class 1 excitable type Izhikevich neuron is used. The firing rates (FR) produced by the neuron in response to different input currents are given in Figure 3. In the inset of Figure 3, it is seen that the neuron can produce spikes when currents above approximately 51.4 μA are applied. To make the model more similar to the ReLu, an external current (51.4 μA) is applied to the model. Additionally, the model is moved to a more appropriate input output space by multiplying the input current I and the firing rate FR by the coefficients p and q, respectively. A similar modulation process has also been shown in the brain in an experimental study with mice [30].

Celal Bayar University Journal of Science
Volume 20, Issue 4, 2024, p 92-100
Doi: 10.18466/cbayarfbe.1538362

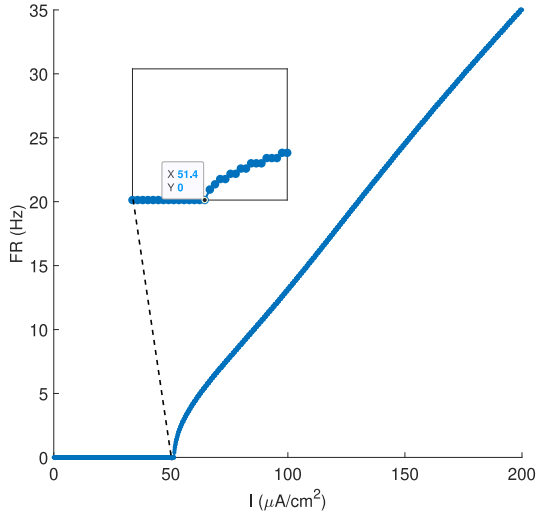

Figure 3. Firing rates of the model

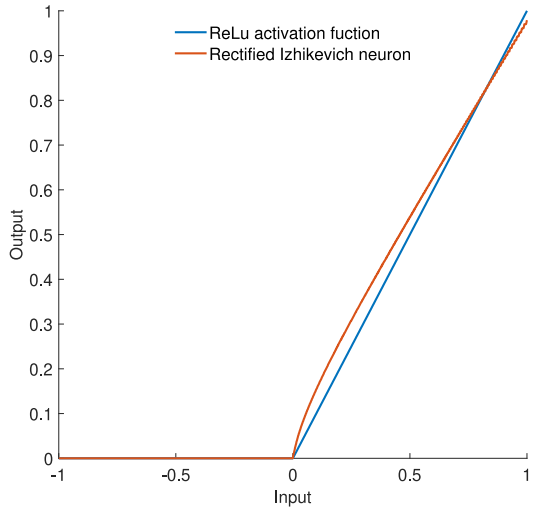

Figure 4. The output of Rectified Izhikevich neuron.

In the study, this model revised with p and q coefficients is called the corrected Izhikevich model. Figure 4 is shown the normalized input and output of the corrected Izhikevich neuron by choosing the p and q values as 10^4 and 10^{-3}, respectively. The FR of the neuron is obtained by calculating the number of spikes produced by the neuron membrane potential in response to the I for 1000 ms using the Euler method.

2.4. Deep Neural Networks

Figure 5 and Figure 6 show the structure of 8 and 4-layer deep neural networks which exhibit ANN or SNN behavior according to the activation mechanism. The neurons that make up the network are activated by ReLu or rectified Izhikevich neurons depending on the mode of the network. In SNN mode, the rectified Izhikevich neuron produces FR as output in response to input, the rectified Izhikevich neuron produces FR as output in response to input I. The data given as a column matrix at the input of the network express the current I. At each layer of the network, the current I from the previous layer is multiplied by the weight w of the network represented by green prisms, normalized by pink prisms, and transformed into a nonlinear form by the activation function represented by blue prisms. The classification result is gained at the softmax output, which is the last layer of the network.

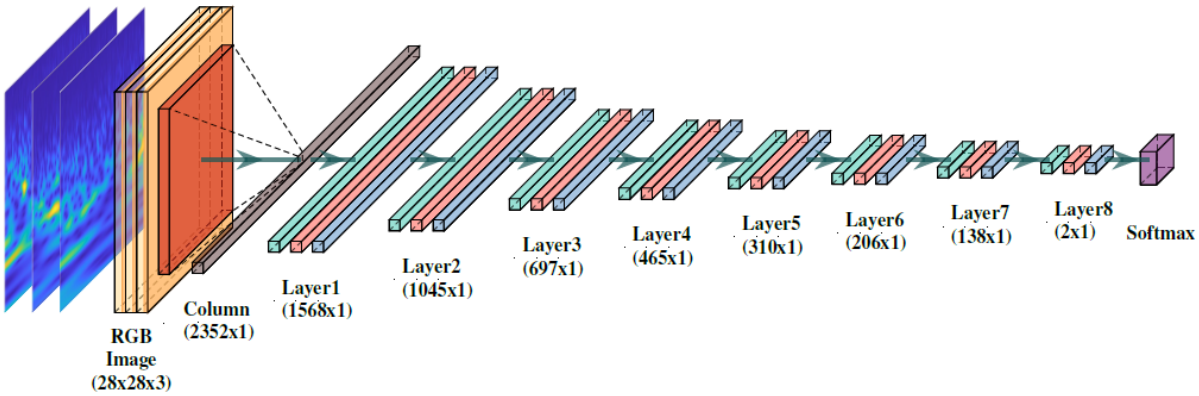

Figure 5. The proposed deep neural network model with 8 layers.

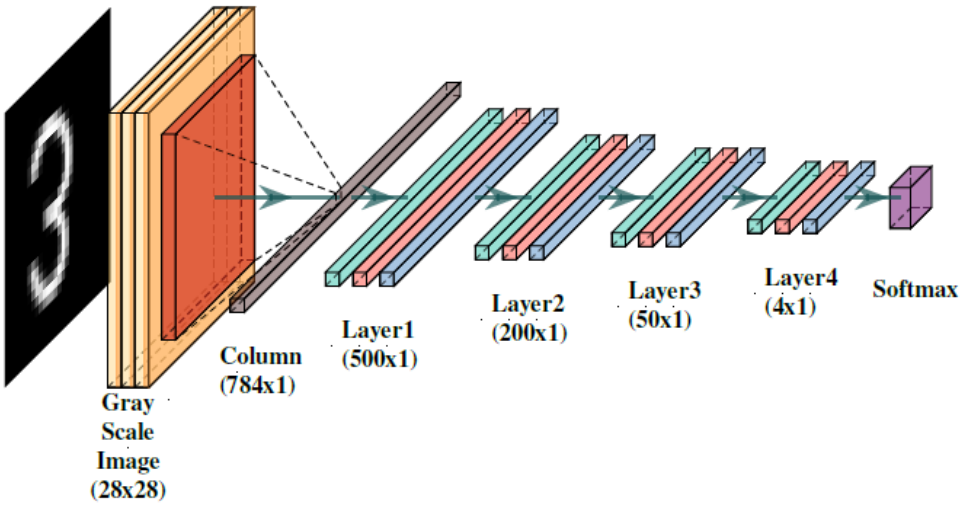

Figure 6. The proposed deep neural network model with 4 layers..

3. Experimental Results

The ECoG and MNIST datasets are classified by using proposed neural networks that can classify in both modes. For the ECoG dataset, the image feature vectors of 28x28x3 are created from the Wavelet scalogram of each trial for the three channels (channel numbers 12, 38, and 29) determined in a previous study [31]. The weights represented by w of the network layers are initially assigned randomly and updated according to the error rate after each iteration. The learning rate α is chosen as $1x10^{-6}$ and $5x10^{-4}$ for ECoG and MNIST datasets, respectively. Experiments are carried out with different learning rates in both types of networks and experiments are continued with the learning rates that achieved optimum classification success. The determined learning rates can be considered as constraints for the study. Experiments are performed in MATLAB 2021b.

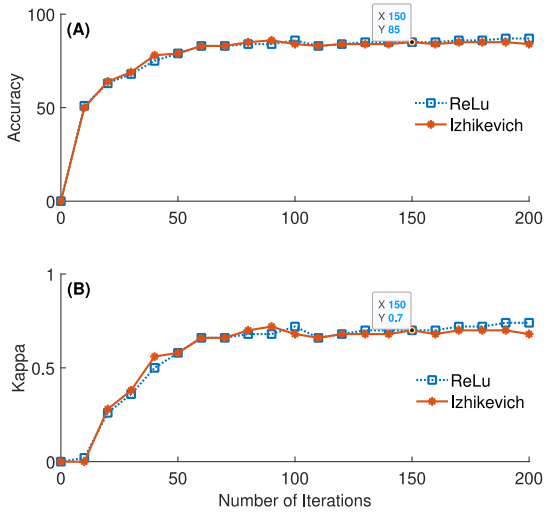

Figure 7. The classification results of the ECoG dataset, (A) accuracies for ANN and SNN modes, (B) Kappa values for ANN and SNN modes ($\alpha = 1x10^{-6}$).

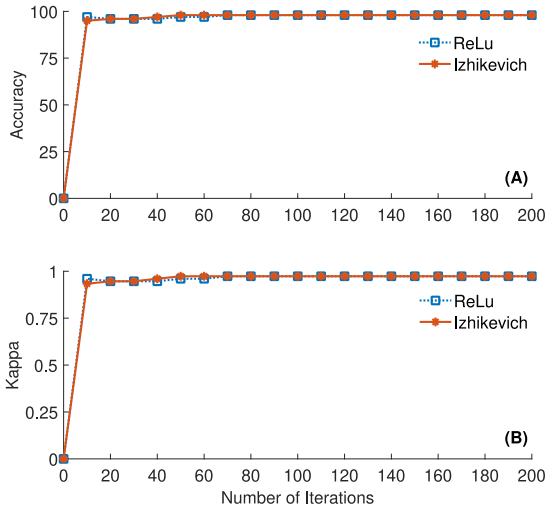

Figure 8. The classification results of the MNIST dataset, (A) accuracies for ANN and SNN modes, (B) Kappa values for ANN and SNN modes. ($\alpha = 5x10^{-4}$)

The classification results are given in Figure 7 A and B, for the ECoG dataset. Figure 7A is shown that the network exhibits similar classification results in SNN and ANN mode. These classification results are supported by Kappa values of 0.70 and above that represent significant classification harmony given in Figure 7 B. Similarly, the MNIST dataset with 4 classes is classified by the ANN mode of the deep neural network given in Figure 6. The high classification result (98%) supported by Kappa value (0.97) is obtained and presented in Figure 8. Classification accuracies and Kappa values for 200 iterations are shown in Figure 8 A and B.

In the first phase of the study, it is seen that 8 and 4-layer deep neural networks are exhibited similar classification results for both modes. One of these parameters is the chaotic current, which is thought to be used in the execution of some cognitive functions in the

Celal Bayar University Journal of Science
Volume 20, Issue 4, 2024, p 92-100
Doi: 10.18466/cbayarfbe.1538362

brain [32]. In line with this idea, in the second stage of the study, 4 different intensities of chaos currents were applied to the rectified Izhikevich neurons in these neural networks to analyze the classification results of the deep SNNs with biological capability in a chaotic environment. The chaotic current applied to the Rectified Izhikevich neuron is demonstrated in Figure 9.

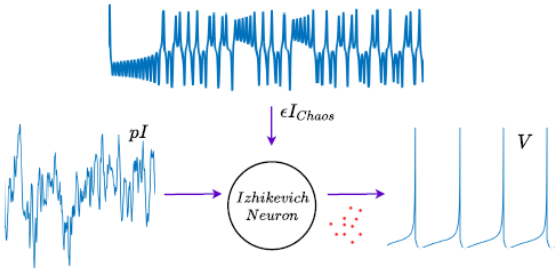

Figure 9. The demonstration of chaotic current on rectified Izhikevich neuron.

This section, it is aimed to investigate the effects of the chaotic environment on the classification performance of the designed SNNs. The average FRs of the rectified Izhikevich neuron as a result of chaotic currents of varying intensity acting on it are shown in Figure 10 in the range $[-1, 1]$. As seen in Figure 10, the consistency of the firing pattern decreases inversely with the chaotic current intensity applied to the neuron. While this consistency is highest with chaos level $\epsilon = 0.001$, it is lowest with chaos level $\epsilon = 0.1$ which represents the highest chaotic current intensity.

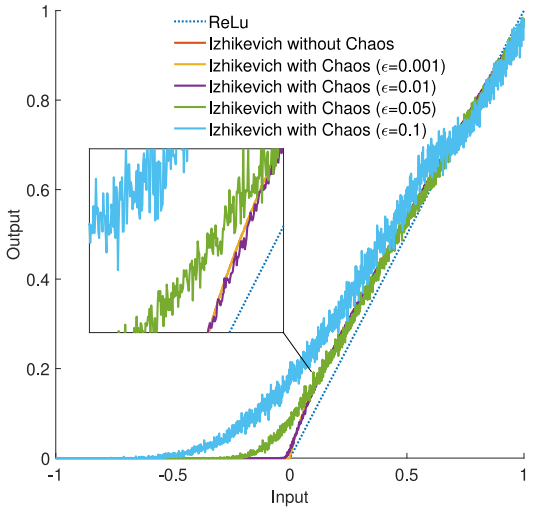

Figure 10. Firing patterns of rectified Izhikevich neuron exposed to different chaotic signal levels.

The classification accuracies, Kappa values, and their average classification accuracies of the SNN consisting of Izhikevich neurons exposed to these different levels of chaotic currents are given in detail in Figure 11, Figure 12, and Table 1, respectively for the ECoG dataset. When both figures and Table 1 are examined, it is seen that the SNNs perform almost the same or even more successful classification compared to an ANN with the same structure activated with the ReLu function, with the selected classification features. More importantly, it has been observed that this classification result is maintained and slightly increased at the optimal chaotic environment level ($\epsilon = 0.01$). It is seen that the classification performance decreases considerably at chaotic current intensities above the optimal level.

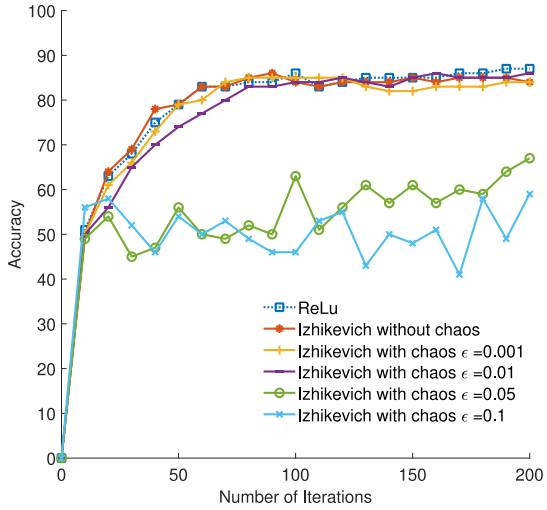

Figure 11. The classification accuracies of the neuron model with ECoG dataset in different level chaos mediums. ($\alpha = 1x10^{-6}$)

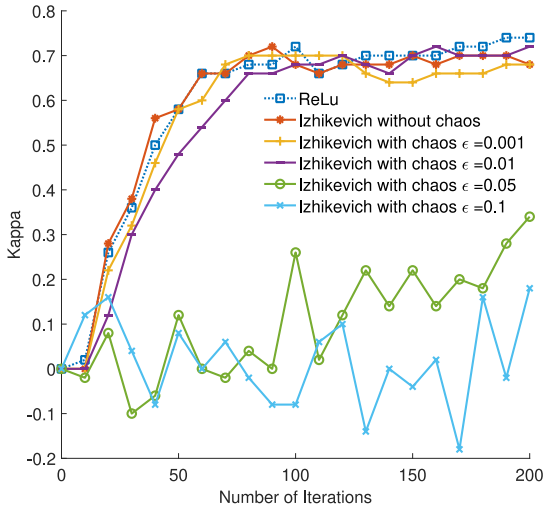

Figure 12. The classification Kappas of the neuron model with ECoG dataset in different level chaos mediums. ($\alpha = 1x10^{-6}$)

Celal Bayar University Journal of Science
Volume 20, Issue 4, 2024, p 92-100
Doi: 10.18466/cbayarfbe.1538362

Table 1. Comparison of overall accuracy for ECoG dataset in different chaotic mediums.

Neuron Type*	Mean Accuracy%	Mean Kappa
ReLu	86.00	0.72
Izhikevich without chaos	84.67	0.69
Izhikevich with chaos ϵ = 0.001	83.17	0.66
Izhikevich with chaos ϵ = 0.01	85.33	0.71
Izhikevich with chaos ϵ = 0.05	61.33	0.23
Izhikevich with chaos ϵ = 0.1	51.00	0.02

Similarly, the classification accuracies, Kappa values, and their average classification accuracies of the SNN consisting of Izhikevich neurons exposed to different levels of chaotic currents are given in detail in Figure 13, Figure 14, and Table 2, respectively for the MNIST dataset. When both figures and Table 2 are examined, results that are in line with the results achieved from the ECoG dataset are obtained. The 4-layer deep neural network given in Figure 6 produced successful results like ANN mode, up to a certain chaotic signal level ($\epsilon = 0.01$) in SNN mode but it could not maintain the classification performance at chaotic levels above $\epsilon = 0.05$. These results are confirmed by the Kappa values given in Figure 14 and the averages given in Table 2.

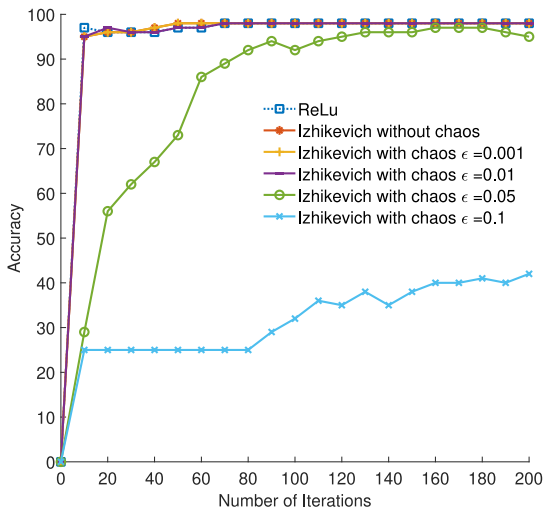

Figure 13. The classification accuracies of the neuron model with MNIST dataset in different level chaos mediums. ($\alpha = 5x10^{-4}$)

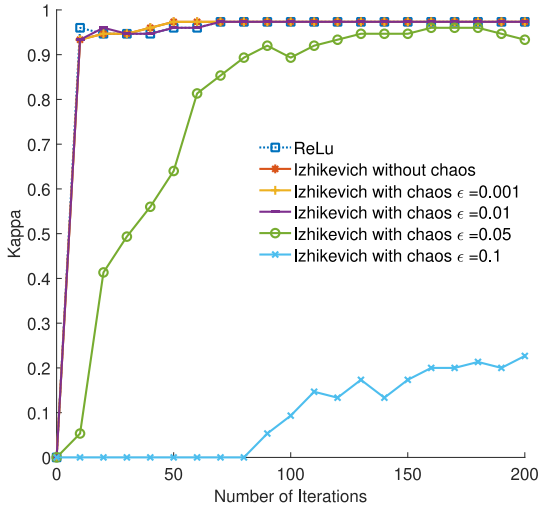

Figure 14. The classification Kappas of the neuron model with MNIST dataset in different level chaos mediums. ($\alpha = 5x10^{-4}$)

Table 2. Comparison of overall accuracy for MNIST dataset in different chaotic mediums

Neuron Type	Mean Accuracy%	Mean Kappa
ReLu	98.00	0.97
Izhikevich without chaos	98.00	0.97
Izhikevich with chaos ϵ = 0.001	98.00	0.97
Izhikevich with chaos ϵ = 0.01	98.00	0.97
Izhikevich with chaos ϵ = 0.05	96.33	0.95
Izhikevich with chaos ϵ = 0.1	40.17	0.20

In Figure 14, classification accuracies of 8 and 4-layer SNNs that classify ECoG and MNIST datasets are given according to the chaotic current levels applied to the neurons in the network. When Figure 15 is examined, it is seen that at a certain chaotic current level ($\epsilon = 0.01$), the classification performance increases slightly, at least the classification performance is preserved. The chaotic current effect is seen more clearly in the classification results of the ECoG dataset. The classification success of the SNN is lower in regions outside the detected chaotic current level ($\epsilon = 0.01$).

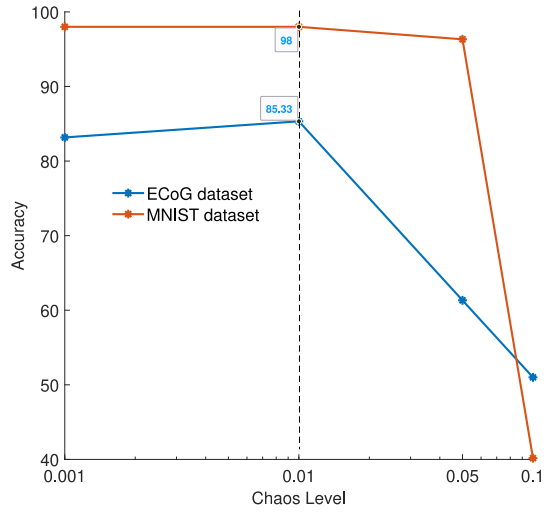

Figure 15. Classification accuracies according to chaotic levels.

4. Conclusion

In the first phase of the paper, neural networks with different layers are designed to perform classifications like ANN and SNN. These neural networks are successfully tested on motor imagery and image datasets. In the first phase of the study, a classification success similar to that of the ANN mode is observed in the SNN mode. In the second stage of the study, starting from the idea that some cognitive brain functions are realized via irregular chaotic neuronal firings [32], the classification performance of the deep SNNs consisted rectified Izhikevich neurons is investigated in different chaotic environments. To the best of our knowledge, the present study is the first to analyze the classification performance of a deep SNN in a chaotic medium. In light of the results obtained, it is seen that the chaotic current applied to the neurons in the network significantly reduces the information processing capability of the network, and this situation is inversely proportional to the intensity of the applied chaotic current. It is noticed that deep SNNs can tolerate the negative effects of chaotic current up to a certain level and even increase the classification performance at some chaotic current levels ($\epsilon = 0.01$). The highest classification accuracies are achieved at this chaotic signal level in both of the data sets used in the study. However, the information processing ability of the SNNs exhibits rapid declines above this value. It is also predicted that a reasonable level of chaotic current will contribute to preventing the overfitting of neural networks. Since the SNNs can express the biological neuron more realistically, these designed SNNs offer the opportunity to investigate the effect of different parameters such as chaotic signals on the neuron. In future studies, it is aimed to investigate similar effects with different data sets on complex neuron models such as Hodgkin Huxley, which better represent the biological neuron.

Author's Contributions

Erdem Erkan: Drafted and wrote the manuscript, performed the experiment and result analysis.

Ethics

There are no ethical issues after the publication of this manuscript.

References

[1]. Rosenblatt, F., 1958. The perceptron: a probabilistic model for information storage and organization in the brain. *Psychological review* 65, 386.

[2]. Abdel-rahman M., George D., Geoffrey H., et al. 2009 Deep belief networks for phone recognition. *In Nips workshop on deep learning for speech recognition and related applications*, volume 1, page 39.

[3]. Krizhevsky A., Sutskever I, and Hinton G.X. 2012 Imagenet classification with deep convolutional neural networks,. *Curran Associates, Inc*., volume 25.

[4]. M. Alfaro-Ponce, A. Arg¨uelles, and I. Chairez. 2016 Pattern recognition for electroencephalographic signals based on continuous neural networks. *Neural Networks*, 79(11):88–96.

[5]. Maass W. 1997 Networks of spiking neurons: the third generation of neural network models. *Neural networks*, 10(9):1659–1671.

[6]. Abbott L.F. 1999 Lapicque's introduction of the integrate-and-fire model neuron (1907). *Brain research bulletin*, 50(5-6):303–304.

[7]. Hodgkin A.L. and Huxley A.F. 1952 A quantitative description of membrane current and its application to conduction and excitation in nerve. *The Journal of physiology*, 117(4):500.

[8]. Izhikevich. E.M. 2004 Which model to use for cortical spiking neurons? *IEEE Transactions on Neural Networks*, 15(5):1063–1070.

[9]. FitzHugh R. 1961 Impulses and physiological states in theoretical models of nerve membrane. *Biophysical journal*, 1(6):445–466.

[10]. Koch C. and Segev I. 1998 Methods in neuronal modeling: from ions to networks. *MIT press*.

[11]. Ghosh-Dastidar S. and Adeli H. 2009 Spiking neural networks. *International journal of neural systems*, 19(04):295–308.

[12]. Kasabov N., Dhoble K., Nuntalid N., and Indiveri G. 2013 Dynamic evolving spiking neural networks for on-line spatio-and spectro-temporal pattern recognition. *Neural Networks*, 41:188–201.

[13]. Dermot Kerr, Sonya Coleman, and Thomas Martin McGinnity. 2018 Biologically inspired intensity and depth image edge extraction. *IEEE Transactions on Neural Networks and Learning Systems*, 29(11):5356–5365

[14]. Carlos D. Virgilio G., Juan H. Sossa A., Javier M. Antelis, and Luis E. Falc´on. 2020 Spiking neural networks applied to the classification of motor tasks in eeg signals. *Neural networks*, 122:130–143.

[15]. Sanders P.J., Doborjeh Z.G., Doborjeh M.G., Kasabov N.K., and Searchfield G.D. 2021 Prediction of acoustic residual inhibition of tinnitus using a brain-inspired spiking neural network model. *Brain Sciences*, 11(1):52.

[16]. Luo Y., Fu Q., Xie J., Qin J., Wu G., Liu J., Jiang F., Cao Y., and Ding X. 2020 Eeg-based emotion classification using spiking neural networks. *IEEE Access*, 8:46007–46016.

[17]. Wu J., Chua Y., and Li H. A biologically plausible speech recognition framework based on spiking neural networks. International Joint Conference on Neural Networks (IJCNN), 2018, pages 1–8. IEEE.

[18]. Wu J., Yılmaz E., Zhang M., Li H., and. Tan. C. K 2020 Deep spiking neural networks for large vocabulary automatic speech recognition. *Frontiers in neuroscience*, 14:199.

[19]. Schmidhuber J. 2015 Deep learning in neural networks: An overview. *Neural networks*, 61:85–117.

[20]. Tavanaei A., Ghodrati M., KheradpishehS.R., Masquelier, and Anthony T. 2019 Deep learning in spiking neural networks. Neural networks, 111:47–63.

[21]. Stiefel K.M., Englitz B., and Sejnowski T.J. 2013 Origin of intrinsic irregular firing in cortical interneurons. *Proceedings of the National Academy of Sciences*, 110(19):7886–7891.

[22]. Rasmussen R., Jensen M.H., and Heltberg M.L. 2017 Chaotic dynamics mediate brain state transitions, driven by changes in extracellular ion concentrations. *Cell systems*, 5(6):591–603.

[23]. Hayashi H., Ishizuka S., and Hirakawa K. 1985 Chaotic response of the pacemaker neuron. *Journal of the Physical Society of Japan*, 54(6):2337–2346.

[24]. Yao Y., Ma J., Gui R, and Cheng G. 2021 Enhanced logical chaotic resonance. Chaos: An *Interdisciplinary Journal of Nonlinear Science*, 31(2):023103.

[25]. Yao Y. and Ma J. 2020 Logical chaotic resonance in a bistable system. International *Journal of Bifurcation and Chaos*, 30(13):2050196.

[26]. Lal T., Hinterberger G., Widman T., Schrder G., Hill J., Rosenstiel W., Elger C., Schlkopf B., and Birbaumer B. 2005 Methods Towards Invasive Human Brain Computer Interfaces. *The MIT Press,*.

[27]. LeCun Y., Bottou L., Bengio Y., and Haffner P. Gradient-based learning applied to document recognition. Proceedings of the IEEE, 1998 86(11):2278–2324.

[28]. Peng Z., Chu F., and He Y. 2002 Vibration signal analysis and feature extraction based on reassigned wavelet scalogram. *Journal of Sound and Vibration*, 253(5):1087–1100.

[29]. Ma J., Ying H., and Pu Z. 2005 An anti-control scheme for spiral under lorenz chaotic signals. *Chinese Physics Letters*, 22(5):1065–1068.

[30]. Beppu K., Kubo N., and Matsui K. 2021 Glial amplification of synaptic signals. *The Journal of Physiology*, 599(7):2085–2102.

[31]. Erkan E. and Kurnaz I. 2017 A study on the effect of psychophysiological signal features on classification methods. *Measurement*, 101:45.-52.

[32]. Hansel D. and Mato G. 2013 Short-term plasticity explains irregular persistent activity in working memory tasks. *Journal of Neuroscience*, 33(1):133–149.